JCI insight

LMAN1 serves as a cargo receptor for thrombopoietin

Lesley A. Everett, … , Beth McGee, Rami Khoriaty

JCI Insight. 2024. https://doi.org/10.1172/jci.insight.175704.

Research In-Press Preview Hematology

Graphical abstract

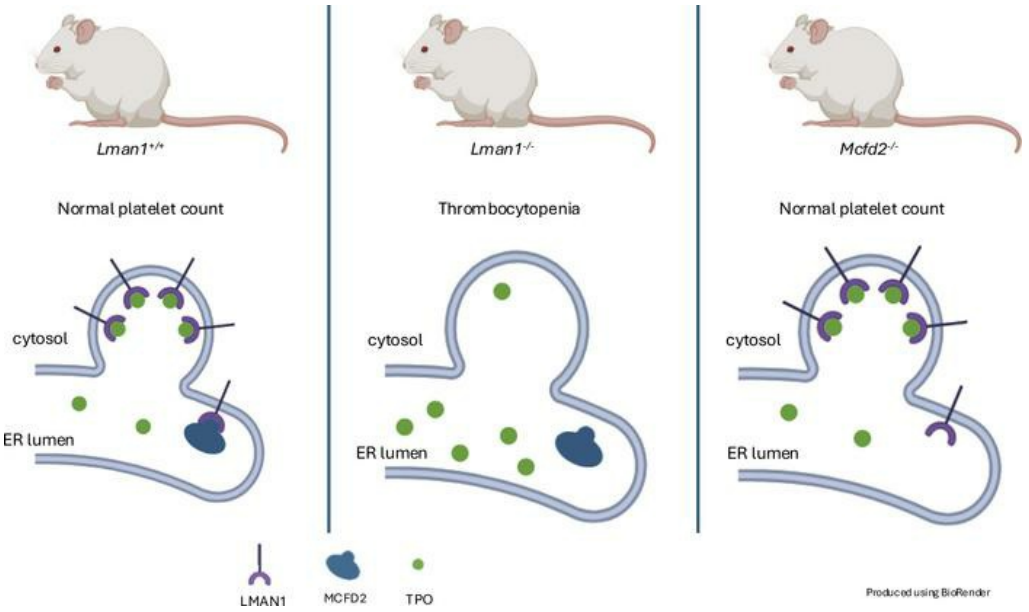

Title:

LMAN1 serves as a cargo receptor for thrombopoietin

Authors:
Lesley A. Everett[1,2], Zesen Lin[3], Ann Friedman[4], Vi T. Tang[5], Greggory Myers[6], Ginette Balbin-Cuesta[7,8], Richard King[4], Guojing Zhu[9], Beth McGee[4], Rami Khoriaty[4,6,7,10*]

1. Department of Ophthalmology, Oregon Health and Science University, Portland, Oregon, USA.
2. Department of Molecular and Medical Genetics, Oregon Health and Science University, Portland, Oregon, USA.
3. Department of Pharmacology, University of Michigan, Ann Arbor, Michigan, USA.
4. Department of Internal Medicine, University of Michigan, Ann Arbor, Michigan, USA.
5. Department of Molecular and Integrative Physiology, University of Michigan, Ann Arbor, Michigan, USA
6. Department of Cell and Developmental Biology, University of Michigan, Ann Arbor, Michigan, USA.
7. Cellular and Molecular Biology Program, University of Michigan, Ann Arbor, Michigan, USA.
8. Medical Scientist Training Program, University of Michigan, Ann Arbor, Michigan, USA.
9. Life Sciences Institute, University of Michigan, Ann Arbor, Michigan, USA.
10. Rogel Cancer Center, University of Michigan, Ann Arbor, Michigan, USA.

* To whom correspondence should be addressed:

Rami Khoriaty, M.D.
BSRB room 1524
109 Zina Pritcher Pl.
Ann Arbor, MI 48109
734-763-3636
ramikhor@umich.edu

Running Title: TPO secretion mediated by LMAN1

Keywords: Thrombopoietin, LMAN1, COPII, endoplasmic reticulum, cargo receptors, megakaryocytes, platelets, SURF4

Conflict of interest: Provisional patent application #63/647,903 (G.M. and R.Kh. co-inventors). Provisional patent application #63/669,963 (R.Kh. co-inventor).

Abstract

Thrombopoietin (TPO) is a plasma glycoprotein that binds its receptor on megakaryocytes (MK) and MK progenitors, resulting in enhanced platelet production. The mechanism by which TPO is secreted from hepatocytes remains poorly understood. LMAN1 and MCFD2 form a complex at the endoplasmic reticulum membrane, recruiting cargo proteins into COPII vesicles for secretion. In this study, we showed that LMAN1 deficient mice (with complete germline LMAN1 deficiency) exhibited mild thrombocytopenia, whereas the platelet count was entirely normal in mice with ~7% *Lman1* expression. Surprisingly, mice deleted for *Mcfd2* did not exhibit thrombocytopenia. Analysis of peripheral blood from LMAN1 deficient mice demonstrated normal platelet size and normal morphology of dense and alpha granules. LMAN1 deficient mice exhibited a trend toward reduced MK and MK progenitors in the bone marrow. We next showed that hepatocyte-specific but not hematopoietic *Lman1* deletion results in thrombocytopenia, with plasma TPO level reduced in LMAN1 deficient mice, despite normal *Tpo* mRNA levels in LMAN1 deficient livers. TPO and LMAN1 interacted by co-immunoprecipitation in a heterologous cell line and TPO accumulated intracellularly in *LMAN1* deleted cells. Altogether, these studies confirmed the hepatocyte as the cell of origin for TPO production *in vivo* and were consistent with LMAN1 as the endoplasmic reticulum cargo receptor that mediates the efficient secretion of TPO. To our knowledge, TPO is the first example of an LMAN1-dependent cargo that is independent of MCFD2.

Introduction

TPO is a plasma glycoprotein that is produced in hepatocytes and regulates platelet production. Circulating TPO binds to its cell surface receptor, MPL, expressed on megakaryocytes (MK) and MK progenitors, promoting cell proliferation and maturation, and enhancing platelet production (1-7). TPO also increases MK ploidy and expression of lineage-specific surface markers (1, 8), and promotes the formation of the demarcation membrane system (precursor to platelet membrane) and platelet granules (7). Consistent with a critical role of TPO in megakaryopoiesis and platelet production, mice with biallelic germline deletion of *Tpo* exhibit a significant reduction in the number of bone marrow (BM) MKs and peripheral blood platelet counts, both to ~10-15% of normal (9), as well as impaired MK maturity (9). In contrast, mice heterozygous for a *Tpo* deleted allele exhibit a ~40% reduction in BM MKs and platelet counts (9, 10), consistent with a dosage effect between the TPO level and MK/platelet numbers.

In addition to its role in MK development and platelet production, TPO also plays a critical role in hematopoietic stem cell (HSC) survival and maintenance (11). TPO deficient mice exhibit a ~70-fold reduction in long-term BM HSCs, although BM cellularity and peripheral blood red blood cell and white blood cell counts remain normal. Mice heterozygous for a *Tpo* null allele exhibit an intermediate phenotype with a ~5-fold reduction in the number of HSCs (11). These and other findings (11, 12) are consistent with a critical role for TPO in HSC maintenance.

In humans, *TPO* mutations that result in enhanced protein translation result in autosomal dominant thrombocytosis (elevated platelet count) (13-18), while loss-of-function mutations in *TPO* (or in its receptor *MPL*) result in congenital amegakaryocytic thrombocytopenia, a disease characterized by thrombocytopenia and absence of BM MKs at birth, with subsequent BM aplasia/failure later in life (19-26). These disorders demonstrate the critical role of TPO in MK and platelet development, as well as in HSC maintenance in humans. Highlighting the role of TPO in platelet production, several TPO-mimetics are FDA-approved for treating certain thrombocytopenia disorders and the bone marrow failure disorder aplastic anemia (27-39).

Plasma TPO levels have been shown to be regulated in part by the rate of plasma clearance. TPO binds its receptor MPL on the platelet surface, resulting in its internalization and destruction (40-42). Additionally, in contrast to earlier reports suggesting that *TPO* mRNA is expressed constitutively and at a steady state (9, 43), aged desialylated platelet removal by the Ashwell-Morell receptor (AMR) was found to result in increased hepatic *Tpo* mRNA production (44), and

GPIbα expressed on the surface of platelets was shown to induce hepatic *TPO* mRNA production in an AMR-independent mechanism (45, 46). Furthermore, inflammatory states also result in increased hepatic *TPO* mRNA production *in vitro* and *in vivo*, an effect mediated by IL-6 (47-51).

Though the transcriptional regulation and plasma clearance of TPO have been well studied, the mechanisms by which TPO is secreted from hepatocytes remains largely unknown. Approximately one third of the mammalian proteome are secretory proteins (52, 53). These proteins are co-translationally translocated into the endoplasmic reticulum (ER) and subsequently transported from ER-to-Golgi via COPII vesicles/tubules before reaching their final destinations (lysosomes, endosomes, plasma membrane, or extracellular space) (54-56). Due to the ER membrane forming a physical barrier between the ER lumen and COPII components, soluble cargoes such as TPO either passively flow into COPII vesicles (bulk flow) or are recruited into COPII vesicles by specific cargo receptors or adaptors (cargo capture) (57-62).

To date, LMAN1 and SURF4 are among the few ER cargo receptors that have been well characterized in mammals (63-74). LMAN1, together with its adapter MCFD2, form a complex that is required for the efficient secretion of coagulation factors V and VIII and alpha1-antitrypsin (65, 70-73). SURF4, on the other hand, promotes the efficient secretion of several other cargos (66-69, 75). Since only a few interactions between soluble cargos and ER receptors have been described in mammals thus far (57, 62, 76), the extent to which bulk flow versus cargo capture contribute to recruitment of proteins in COPII vesicles is unclear.

We now report that LMAN1 deficient, but not MCFD2-deficient mice, exhibit thrombocytopenia and that mice with combined deficiency of LMAN1 and MCFD2 exhibit thrombocytopenia indistinguishable from that in LMAN1 deficient mice. Tissue-specific deletion of *Lman1* results in thrombocytopenia in mice with hepatocyte-specific *Lman1* deletion but not in mice with deletion of *Lman1* in hematopoietic cells. Plasma TPO level (but not liver *Tpo* mRNA) is reduced in *Lman1* null mice, with evidence for TPO and LMAN1 physical interaction in heterologous cells *in vitro*, as well as intracellular accumulation of TPO in LMAN1 deficient cells. Taken together, these results identify TPO as a likely cargo for the ER cargo receptor, LMAN1.

Results

LMAN1 deficient mice are thrombocytopenic

We previously generated mice with a conditional *Lman1* allele (*Lman1*^{fl}), in which exons 2 and 3 are flanked by LoxP sites (Fig.1A) (77). We crossed the *Lman1*^{fl} allele to a mouse expressing Cre-recombinase under the control of the *EIIa* promoter, resulting in germline deletion of exons 2 and 3, a frameshift mutation, and a null *Lman1* allele (*Lman1*$^{-}$) (Fig.1A). In the current study, we examined complete blood counts in samples obtained from *Lman1* null mice. Surprisingly, *Lman1*$^{-/-}$ mice exhibited a ~30% reduction in platelet count relative to wildtype (WT) littermates ($p<0.0005$) (Fig. 1B). The mean platelet volume was normal in *Lman1*$^{-/-}$ mice (Fig. 1C) and no other abnormality on complete blood count analysis was found (Fig. 1 D-E).

Hypomorphic *Lman1* mice are not thrombocytopenic

Mice heterozygous for the *Lman1*$^{-}$ allele (*Lman1*$^{+/-}$ mice), with 50% *Lman1* expression, exhibited normal platelet counts compared to WT littermate controls (Fig. 1F). We previously reported the generation of mice carrying a hypomorphic *Lman1* allele resulting in *Lman1* expression at ~7% of wild type levels (*Lman1*^{cgt}) (77). To determine if reduced *Lman1* expression to ~7% of normal results in thrombocytopenia, we now analyzed complete blood counts in blood samples obtained from the latter mice. We found that *Lman1*$^{cgt/cgt}$ mice, which express ~7% of normal *Lman1* levels, exhibited normal platelet counts indistinguishable from wildtype litter mate controls (Fig. 1F). These results demonstrate that the thrombocytopenia is only evident with complete LMAN1 deficiency.

MCFD2 deficient mice do not exhibit thrombocytopenia

LMAN1 and MCFD2 form a cargo receptor complex at the ER membrane. Secretory proteins including factor V, factor VIII, and α1-antitrypsin, that depend on LMAN1 for secretion, have been shown to also depend on LMAN1's adaptor, MCFD2, for efficient secretion. To determine if MCFD2 deficient mice exhibit thrombocytopenia similar to LMAN1 deficient mice, we generated mice that are homozygous for our previously described *Mcfd2* deleted allele (*Mcfd2*$^{-/-}$) (78) (Fig. 2A). Surprisingly, in contrast to *Lman1*$^{-/-}$ mice, we found that *Mcfd2*$^{-/-}$ mice exhibited normal platelet counts (Fig. 2 B).

Next, we intercrossed *Lman1 Mcfd2* double heterozygous mice to generate mice with combined

LMAN1/MCFD2 deficiency. Consistent with the earlier data, analysis of singly deficient mice confirms the previously noted mild thrombocytopenia in *Lman1*$^{-/-}$ mice (with average platelet count ~70% of wildtype) with normal platelet counts in MCFD2 deficient mice. LMAN1/MCFD2 double deficient mice exhibit thrombocytopenia, with platelet counts indistinguishable from *Lman1*$^{-/-}$ mice (Fig. 2C). Taken together, these results suggest that the thrombocytopenia observed in *Lman1*$^{-/-}$ mice results from a novel LMAN1-specific (but MCFD2 independent) function, affecting MK/platelet differentiation and/or survival.

MK and platelet morphology in LMAN1 deficient mice

To define the role of LMAN1 in MK/platelet development or survival, additional studies were performed. Peripheral smears demonstrated normal platelet size and morphology in *Lman1*$^{-/-}$ mice (Fig. 3A). Next, transmission electron microscopy showed no difference in platelet size or in morphology of dense or alpha granules between *Lman1*$^{-/-}$ and WT mice, as evaluated by 2 observers blinded to the mouse genotype (Fig. 3B). Additionally, histologic examination of *Lman1*$^{-/-}$ and WT femurs by 2 observers blinded to mouse genotype detected no difference in MK morphology between both genotypes (Fig. 3C), but a trend towards reduced number of MKs in *Lman1*$^{-/-}$ compared to WT BMs was noted (Table S1). Furthermore, bone marrow analysis by flow cytometry similarly demonstrated a trend (albeit non-significant) towards reduced MK progenitors ($Lin^{-}Sca^{-}KIT^{+}CD150^{+}CD41^{+}$) in LMAN1 deficient mice (Fig. 3 D-E and Fig. S1), with no effect on hematopoietic stem cells or early progenitors (Fig. S2 A-F).

***Lman1* deletion in hepatocytes, but not hematopoietic cells, results in thrombocytopenia**

To determine whether the thrombocytopenia results from LMAN1 deficiency specifically in the hematopoietic compartment, mice with tissue-specific knockout of *Lman1* in hematopoietic and endothelial cells were generated by crossing the *Lman1*^{fl} allele to the *Tie2*-Cre transgene (Fig. 4A) (Table 1). To our surprise, platelet counts of mice with hematopoietic LMAN1 deficiency were comparable to those of WT littermate controls (Fig. 4B). Thus, the thrombocytopenia observed in *Lman1*$^{-/-}$ mice is not due to a defect intrinsic to MK, platelets, or a hematopoietic cell.

We subsequently generated mice with *Lman1* deletion exclusively in the hepatocytes by crossing the *Lman1*^{fl} allele to the *Alb*-Cre transgene (Fig. 4A) (Table 1). Mice with *Lman1* deletion restriced to hepatocytes exhibited significant thrombocytopenia relative to WT controls ($p<0.017$) (Fig. 4B), with platelet counts indistinguishable from those in ubiquitous *Lman1* null mice. These data

suggest the presence of a novel LMAN1-dependent secretory cargo synthesized in the hepatocyte that contributes to the regulation of platelet count in mice.

Deletion of Surf4 in hepatocytes does not result in thrombocytopenia

We additionally generated and analyzed mice with hepatocyte-specific deletion of *Surf4*, an ER cargo receptor that has been shown to regulate the secretion of several mammalian proteins, including PCSK9, erythropoietin, and others (66-69). In contrast to mice with hepatocyte-specific *Lman1* deletion, mice with deletion of *Surf4* in hepatocytes did not exhibit thrombocytopenia (Figure S3 A-D), suggesting that SURF4, unlike LMAN1, does not play a role in the secretion of TPO under steady state conditions.

Plasma TPO level is reduced in LMAN1 deficient mice

Since TPO is a major hepatocyte-derived regulator of platelet synthesis, we reasoned that TPO production, stability, or secretion could be impaired in *Lman1*$^{-/-}$ mice, resulting in thrombocytopenia. Measurement of plasma TPO levels by ELISA demonstrated a reduction in *Lman1*$^{-/-}$ mice compared to WT controls ($120x10^3$ vs. $230x10^3$ pg/mL, respectively, $p<0.0024$) (Fig. 5A). However, *Tpo* mRNA levels were indistinguishable between *Lman1*$^{-/-}$ and WT livers (Fig. 5B). LMAN1-FLAG and TPO-myc co-expressed in HEK293T cells appear to physically interact, as demonstrated by co-immunoprecipitation of TPO with an anti-FLAG antibody (Fig. 5C). In contrast, MCFD2 and TPO do not appear to physically interact by co-immunoprecipitation (Fig S4).

Finally, co-expression of TPO fused to eGFP and A1AT fused to mCherry in HEK293 cells demonstrated increased intracellular accumulation of both proteins following deletion of *LMAN1*, consistent with the known dependence of A1AT on LMAN1 for secretion and suggesting a similar dependence for TPO (Fig. 5D). Notably, *LMAN1* deletion resulted in significantly increased localization of TPO in the ER ($p<0.0001$) (Fig 5E). Similarly, a separate reporter cell line expressing TPO fused to mCherry, and as negative control PCSK9 fused to GFP, demonstrated intracellular accumulation of TPO in *LMAN1* deleted cells, with no effect on PCSK9 secretion (Fig. 5F). Importantly, *LMAN1* deletion in the human hepatocyte cell line HEP3B, which expresses TPO from its endogenous locus, resulted in reduced secreted TPO in the media (Fig 5G). Taken together, these findings demonstrate that LMAN1 is the ER cargo receptor that is required for efficient TPO secretion.

Lman1 null mice exhibit delayed platelet recovery under hematopoietic stress

We next investigated if LMAN1 deficiency results in impaired platelet recovery under stress. We exposed *Lman1*$^{-/-}$ and wildtype litter mate contro mice to chemotherapy (fluorouracil, 5-FU) and measured platelet count recovery over time. Platelet recovery was significantly delayed in *Lman1* null mice (Fig S5).

Discussion

LMAN1 is a transmembrane protein localized to the ER membrane that together with MCFD2, forms a receptor complex facilitating the secretion of coagulation factors V and VIII. Loss of function mutations in *LMAN1* (or in *MCFD2*) cause the rare autosomal recessive bleeding disorder, combined factor V and VIII deficiency (F5F8D), characterized by reduced plasma levels of these two clotting factors to ~10% of normal due to their impaired secretion. The fact that the *LMAN1* gene appeared in evolution before the existence of coagulation factors V and VIII suggests that there are additional LMAN1-dependent cargos (or other functions for LMAN1); however, to date, only a handful of cargos have been shown to depend on LMAN1 for secretion.

In this report, we show that: i) mice deficient in LMAN1 exhibit thrombocytopenia; ii) mice with hepatocyte-specific *Lman1* deletion exhibit thrombocytopenia, while mice with hematopoietic-specific *Lman1* deletion do not; iii) plasma TPO level is reduced in *Lman1*$^{-/-}$ compared to WT littermate controls; iv) TPO mRNA is unchanged in *Lman1*$^{-/-}$ hepatocytes; v) TPO protein accumulates intracellularly in LMAN1 deficient cells; and vi) TPO and LMAN1 physically interact. Collectively, these results, taken together with LMAN1's known function as an ER cargo receptor, strongly suggest that the thrombocytopenia observed in *Lman1*$^{-/-}$ mice is due to impaired secretion of TPO from hepatocytes. The normal platelet volume observed in *Lman1*$^{-/-}$ mice is consistent with the generally normal platelet size in patients with congenital thrombocytopenia resulting from a defect in TPO/TPO receptor signaling (79).

In contrast to coagulation factors V and VIII and alpha1-antitrypsin (65, 70-73) which require both LMAN1 and MCFD2 for efficient exit from the ER, our results suggest that TPO depends on LMAN1 but not MCFD2 for secretion, the first example of an LMAN1-dependent cargo protein that is independent of MCFD2. TPO could interact with LMAN1 either directly or indirectly via an adaptor other than MCFD2, though no such alternative LMAN1 adaptor proteins have yet been identified. Additionally, while a dose response relationship between secretion levels of other LMAN1-dependent cargos and Lman1 expression levels was demonstrated (77), the same does not appear to be the case for TPO.

Of note, patients with combined deficiency for coagulation factors V and VIII have not been reported to exhibit thrombocytopenia. Though the mean platelet count varies widely among different inbred mouse strains, the standard deviation for platelet count measurements within a single inbred mouse strain such as C57BL6/J as studied here, is only ~10%, affording statistical

power to detect subtle difference in platelet count between control and experimental groups even when the sample size is small. In contrast, platelet counts vary considerably among humans and may fluctuate dramatically within the same individual in various settings. Therefore, we hypothesize that the relatively subtle degree of thrombocytopenia detected in our LMAN1 null mice would likely be missed among the diverse population of human F5F8D patients, particularly given that a 20-30% reduction in platelet count is still well within the normal range. It is also possible that the magnitude of the change in TPO secretion and corresponding platelet count reduction is more subtle in human than in mice. Though we cannot exclude the possibility that TPO is dependent on LMAN1 for efficient secretion in mice but not in humans, our observation that intracellular accumulation of TPO also occurs in a human cell line following deletion of *LMAN1* suggests a similar process in both species.

The primary site of TPO production has been a longstanding controversy. *TPO* mRNA expression has been reported in various tissues including liver, spleen, kidney, BM, mesenchymal stromal cells, and osteoblasts (11, 80-86). However, the translation of *TPO* mRNA to protein is under stringent control by inhibitory elements in the 5' untranslated region (87), which limits the cell type(s) that produce the TPO protein. Indeed, recent work using genetically engineered mice that report the expression of TPO at the protein level demonstrated absence of TPO protein expression in most cells types that had been previously implicated in TPO production (except for the liver) (11). Consistent with these results, conditional deletion of *Tpo* from osteoblasts, Lepr+ mesenchymal stromal cells, or BM cells, resulted in no hematopoietic defects (11). In contrast, hepatocyte-specific *Tpo* deletion (*Alb*-Cre) resulted in hematopoietic defects indistinguishable from those in mice with germline *Tpo* deletion (11). Similarly, *Tpo* deletion in hepatocytes of adult mice also resulted in decreased platelet production (11). These results demonstrate that hepatocytes are the physiological source of TPO both during development and in adult life. Consistent with these findings, liver transplantation for liver cirrhosis results in increased plasma TPO levels 1 day post-transplantation, with a subsequent increase in platelet count (88). This report further supports the hepatocyte as the cell of origin for TPO production.

The findings reported here may lay the foundation for the development of new strategies to therapeutically alter plasma TPO level, with potential applications for the treatment of disorders of both low and high platelet counts.

Methods

Sex as a biological variable

Our study included male and female mice, and similar findings are found for both sexes.

Lman1 and *Mcfd2* mutant mice

Hypomorphic *Lman1*$^{cgt/cgt}$ mice with a gene-trap insertion in inton 1 of *Lman1* were described previously (89). An *Lman1* floxed allele (*Lman1*^{fl}) in which exons 2 and 3 are flanked by LoxP sites was generated by crossing the *Lman1*^{cgt} allele to a mouse expressing FLPe recombinase from an actin promoter (Jackson Laboratory stock no. 003800) as previously described (89). Crossing the *Lman1*^{fl} allele to mice expressing Cre-recombinase under the control of the EIIa promoter (*EIIa*-Cre, Jackson Laboratory stock no. 003724) results in germline excision of exons 2 and 3 and a germline null *Lman1* allele (*Lman1*$^{-}$). Mice heterozygous for the *Lman1*$^{-}$ allele (*Lman1*$^{+/-}$) were backcrossed to C57BL/6J mice to achieve germline transmission of the *Lman1*$^{-}$ allele. The resulting *Lman1*$^{+/-}$ mice were intercrossed to generate mice with germline homozygous deletion of *Lman1* (*Lman1*$^{-/-}$). The *Mcfd2* null allele (*Mcfd2*$^{-}$) with deletion of exons 2 and 3 was also generated as previously described(78). Mice with germline biallelic deletion of Mcfd2 (*Mcfd2*$^{-/-}$) were generated by intercrossing *Mcfd2*$^{+/-}$ mice. All *Lman1* and *Mcfd2* alleles were backcrossed to C57BL/6J mice for more than 8 generations and subsequently maintained on the C57BL/6J genetic background. *Lman1*$^{-/-}$ and wildtype littermate control mice were administered fluorouracil (5-FU, Fresenius Kabi USA, product #101720) at 150 mg/Kg body weight once, to induce hematopoietic stress. Platelet counts were measured on days 3, 6, 9, 11, and 15 post chemotherapy administration.

Tissue specific *Lman1* and *Surf4* deletion

Mice heterozygous for the *Lman1*^{fl} allele (*Lman1*$^{+/fl}$) were crossed to mice expressing Cre recombinase under the control of the *Albumin* promoter (*Alb*-Cre^{+} mice) (Jackson Laboratory stock number 003574 (90)). *Lman1*$^{+/fl}$ *Alb*-Cre+ mice generated from the latter cross were subsequently crossed to *Lman1*$^{+/fl}$ mice to generate mice with hepatocyte-specific *Lman1* deletion (*Lman1*$^{fl/fl}$ *Alb*-Cre+ mice). Using a similar strategy, mice with deletion of *Lman1* in *Tie2*-expressing endothelial and hematopoietic cells (*Lman1*$^{fl/fl}$ *Tie2*-Cre+ mice) were generated, using the previously reported *Tie2*-Cre allele (Jackson Laboratory stock number 004128 (91)).

Mice heterozygous for a *Surf4* floxed allele (*Surf4*$^{+/fl}$) were generated as previously described (92), and mice with hepatocyte-specific *Surf4* deleion (*Surf4*$^{fl/fl}$ *Alb*-Cre+ mice) were generated as summarized above.

Mouse genotyping

Genomic DNA was extracted from mouse tail biopsies as previously described. Genotyping for the *Lman1*^{fl}, *Lman1*$^{-}$, *Lman1*^{cgt}, *Mcfd2*$^{-}$, *Surf4*^{fl}, *Alb*-Cre and *Tie2*-Cre alleles was performed as previously described (78, 89, 93).

Complete blood counts

Mice were anesthetized briefly with isoflurane and blood was collected from the retro-orbital venous sinuses as previously described (94). Complete blood count analysis was performed as previously described (95).

Bone marrow histology and flow cytometry

Femurs from *Lman1*$^{-/-}$ and WT control adult mice were harvested to assess bone marrow cellularity and architecture as well as numbers of megakaryocyte per bone marrow section. Samples were processed, embedded, sectioned, and stained at the University of Michigan Animal Research Facility. Femurs were fixed in 10% neutral buffered formalin prior to processing, and bones were decalcified in Immunocal (Decal Chemical Corporation) for 24 hours.

Anesthetized mice were euthanized, and bone marrow was flushed from femurs and tibias using RPMI 1640 (Sigma-Aldrich) supplemented with 5% FBS. Bone marrow cells were stained with combinations of the following antibodies: anti-SCA1 (BioLegend 108128 or 108127), anti-cKIT (BioLegend 105826), anti-CD150 (BioLegend 115913 or 115914), anti-CD105 (Biolegend 120403 with secondary antibody staining using Biolegend 405232), anti-CD48 (BioLegend 103404), anti-CD41 (BioLegend 133925), anti-CD16/32 (BioLegend 101314), as previously described(96). A Lineage cocktail consisted of the following antibodies: anti-CD3 (BioLegend 100307 or 100308), anti-CD8 (BioLegend 100708), anti-CD4 (Biolegend 116006) anti-CD11b (BioLegend 101208), anti-CD11c (BioLegend 117308), anti-CD19 (BioLegend 115508 or 557399), anti-B220 (BioLegend 103208), anti-TCR-B (BioLegend 109208), anti-TCR-YD (BioLegend 118108), anti-Gr1 (BioLegend 108408), anti-NK1.1 (BioLegend 108708). DAPI (Sigma-Aldrich #D8417) or

Zombie Aqua Fixable Viability Dye (Biolegend 423102) was used to distinguish dead from live cells. Analysis was performed using FlowJo software (BD Life Sciences).

Electron microscopy

Platelet-rich plasma and platelet pellets were isolated and processed as follows. Two milliliters of room temperature Buffered Saline Glucose Citrate (BSGC) (129 mM NaCl, 13.6 mM Na_3 citrate, 11.1 mM glucose, 1.6 mM KH_2PO_4, 8.6 mM NaH_2PO_4, pH 7.3) were placed in a 5 mL polypropylene tube, to which 1-1.5 mL of whole blood was added. BSGC was added to a final volume of 4 mL. The tubes were gently mixed by inversion and were centrifuged at 180 x g for 10 minutes at room temperature without brake. The supernatants (semi-platelet rich plasma) were removed and centrifuged in fresh tubes at 700 x g for 10 minutes with brake. The resulting isolated platelet pellets were resuspended and prepared for electron microscopy as previously described(95). Briefly, platelet pellets were fixed overnight at 4°C in 0.1 M Sorensen's buffer (0.1 M Na_2HPO_4, 0.1 M KH_2PO_4, pH 7.4) containing 2.5% glutaraldehyde. Subsequently, and in this order, platelets were rinsed in 0.1 M Sorensen's buffer, fixed with 1% osmium tetroxide in 0.1 M Sorensen's buffer, rinsed in double distilled water, and then stained *en bloc* with aqueous 3% uranyl acetate for 1 hour. Platelets were dehydrated in ascending concentrations of ethanol, rinsed twice in 100% ethanol, and embedded in epoxy resin. Sample processing and transmission electron microscopy (TEM) was performed at the University of Michigan Microscopy & Image Analysis Laboratory. Samples were ultra-thin sectioned at 70 nm thickness and stained with uranyl acetate and lead citrate. TEM was performed using a Philips CM100 electron microscope at 60kV. Images were recorded digitally using a Hamamatsu ORCA-HR digital camera system operated with AMT software (Advanced Microscopy Techniques Corp., Danvers, MA).

qRT-PCR

Total mRNA was prepared from livers isolated from adult WT and *Lman1*$^{-/-}$ mice, and cDNA synthesis was performed (with on column DNAseI digestion) as previously described(97). qRT-PCR was performed with SYBR-Green RT-PCR Master Mix (Applied Biosystems) using primers listed in Table S2 on a 7900HT Fast Real-Time PCR machine (Applied Biosystems). Data were analyzed using the $2^{-\Delta\Delta CT}$ method as previously described(98), using GAPDH and actin as control.

Co-immunoprecipitation

Mammalian vectors that express FLAG-fused LMAN1 (LMAN1-FLAG) and Myc-fused TPO (TPO-Myc) were generated and transfected in HEK293T cells using Fugene HD transfection reagent (Promega), per manufacturer's instructions. LMAN1 immunoprecipitation was performed using anti-FLAG antibody covalently bonded to agarose beads (EZview Red Anti-FLAG M2 affinity gel, Sigma-Aldrich). Immunoblotting with anti-myc antibody (ab10312, Abcam Inc) was performed as previously described(95). To test if MCFD2 physically interacts witih TPO, we overexpressed MCFD2-FLAG in HEK293T cells that express TPO-eGFP. Fourty eight hour post-transfection, MCFD2 immunoprecipitation was performed using anti-FLAG M2 magnetic beads (Sigma, M8823), followed by immunoblotting with anti-eGFP antibody (abcam, ab290). TPO immunoprecipitation was also performed using chemoTek GFP-Trap Magnetic Agarose (Proteintech, cat # gtma) followed by anti-FLAG immunoblotting (Abcam, ab1238).

Generation of a TPO reporter cell line

A construct (CMV-PCSK9-eGFP-p2A-TPO-mCherry) that expresses PCSK9 fused to eGFP and TPO fused to mCherry from the CMV promoter was assembled as previously described (99). HEK293T cells were transfected with this construct using Fugene HD transfection reagent (Promega) and transfected cells were selected with hygromycin (Invitrogen) for five weeks. Single cells were subsequently sorted into 96-well plates using SY-3200 flow cytometry (Sony). A clonal cell line that stably expresses PCSK9-GFP and TPO-mCherry was established. Similarly, a construct (CMV-TPO-eGFP-p2A-A1AT-mCherry) was used to generate a clonal cell line that stably expresses TPO-eGFP and A1AT-mCherry.

LMAN1* deletion *in vitro

An sgRNA targeting *LMAN1* (5'-GATGTGGCAACGCGACCGCG-3') was generated and cloned into the pLentiCRISPRv2 plasmid (Addgene no. 52961, a gift from Feng Zhang). To prepare lentivirus, pLentiCRISPRv2 was co-transfected with pxPAX2 (Addgene no. 12260, a gift from Didier Trono) and pCMV-VSV-G (Addgene no. 8454, a gift from Robert Weinberg) in a 2:1.5:1 ratio into HEK293T cells at ~80% confluence, using Fugene HD transfection reagent (Promega). Twenty-four hours post-transfection, the medium was changed, and viral supernatant was collected 24 hours later. Media containing viral supernatant was centrifuged at 500x g for 5 minutes, aliquoted, snap-frozen in liguid nitrogen, and stored at -80°C. pLentiCRISPRv2 Lentiviral particles expressing non-targeting control sgRNA were also generated as above. To delete *LMAN1*, cells were transduced with pLentiCRISPRv2 lentivirus expressing an *LMAN1*-targeting

sgRNA at a multiplicity of infection of ~0.3. Transduced cells were selected with puromycin for 4 days, and analysis was performed ~10 days afterwards.

Live confocal microscropy

Repoter HEK293T cells that express TPO-eGFP and A1AT-mCherry were transduced with *LMAN1* targeting sgRNA (listed above) or non-targeting control sgRNA. The latter cells were subsequently transfected with a plasmid expressing ERoxGFP (addgene no. 68126, a gift from Erik Snapp (100)). Twenty four hours post-transfection, cells were seeded on Lab-Tek Chambered Coverglass (ThermoFisher). Using Nikon IR fluorescence microscope, images were captured. Pearson correlation coefficient was measured using the Nikon elements software to analyze the colocalization between TPO and the ER.

TPO elisa

Murine plasma TPO levels were measured by Elisa (MTP00, R&D system) per manufacturer's instructions. Secreted TPO was also measured in media of HEP3B cells treated with 80 ng/mL IL-6 (Thermo Fisher 200-06) for 24 hours, using Human Thrombopoietin Quantikine ELISA kit (Fisher DTP00B) per manufacturer's instructions. Results were normalized to cell counts, assessed by the MTT assay (Roche #11465007001) per manufacturer's instructions.

Study approval

All experiments utilizing mice were performed in accordance with the regulations of the University Committee on Use and Care of Animals.

Statistical analysis

When two groups are compared, data was analyzed using 2-tailed unpaired Student's t-test. When three or more groups are compared, data was compared using one-way ANOVA, with correction for multipe comparison testing. A p-value less than 0.05 was considered statistically significant.

Data availability

Lman1 and Mcdf2 mutant mice are available at the Jackson laboratory (#068108-JAX and #024426, respectively). Supporting data values are included in a supplemental document.

Acknowledgments

L.E. and R.Kh. conceived the study and designed the experiments. L.E. and R.Kh. performed the majority of the experiments. Z.L., A.F., V.T.T., G.M., G.B.C., R.Ki, G.Z., and B.M. performed additional experiments. L.E.and R.Ki. analyzed most of the experimental data. L.E. and R.Kh. wrote the manuscript with help from all authors. All the authors contributed to the integration and discussion of the results. The authors declare that they have no competing interests. All data needed to evaluate the conclusions in the paper are present in paper and/or the Supplementary Materials. This work was supported by a National Institute of Health Grant R01 HL 157062 (R.Kh.), R01 HL148333 (R.Kh.), and R35 HL 135793 supporting V.T.T., G.Z., and B.M. This work was also supported by The University of Michigan Rogel Cancer Center P30CA046592 grant (providing support for R.Kh.). R.Ki. was supported by NIH T32-CA009357. G.B.C. was supported by NIH T32-GM007315 and F31HL162544.

References

1. Kaushansky K, Lok S, Holly RD, Broudy VC, Lin N, Bailey MC, et al. Promotion of megakaryocyte progenitor expansion and differentiation by the c-Mpl ligand thrombopoietin. *Nature.* 1994;369(6481):568-71.
2. de Sauvage FJ, Hass PE, Spencer SD, Malloy BE, Gurney AL, Spencer SA, et al. Stimulation of megakaryocytopoiesis and thrombopoiesis by the c-Mpl ligand. *Nature.* 1994;369(6481):533-8.
3. Lok S, Kaushansky K, Holly RD, Kuijper JL, Lofton-Day CE, Oort PJ, et al. Cloning and expression of murine thrombopoietin cDNA and stimulation of platelet production in vivo. *Nature.* 1994;369(6481):565-8.
4. Bartley TD, Bogenberger J, Hunt P, Li YS, Lu HS, Martin F, et al. Identification and cloning of a megakaryocyte growth and development factor that is a ligand for the cytokine receptor Mpl. *Cell.* 1994;77(7):1117-24.
5. Kuter DJ, Beeler DL, and Rosenberg RD. The purification of megapoietin: a physiological regulator of megakaryocyte growth and platelet production. *Proc Natl Acad Sci U S A.* 1994;91(23):11104-8.
6. Sohma Y, Akahori H, Seki N, Hori T, Ogami K, Kato T, et al. Molecular cloning and chromosomal localization of the human thrombopoietin gene. *FEBS Lett.* 1994;353(1):57-61.
7. Kaushansky K, Broudy VC, Lin N, Jorgensen MJ, McCarty J, Fox N, et al. Thrombopoietin, the Mp1 ligand, is essential for full megakaryocyte development. *Proc Natl Acad Sci U S A.* 1995;92(8):3234-8.
8. Zeigler FC, de Sauvage F, Widmer HR, Keller GA, Donahue C, Schreiber RD, et al. In vitro megakaryocytopoietic and thrombopoietic activity of c-mpl ligand (TPO) on purified murine hematopoietic stem cells. *Blood.* 1994;84(12):4045-52.
9. de Sauvage FJ, Carver-Moore K, Luoh SM, Ryan A, Dowd M, Eaton DL, et al. Physiological regulation of early and late stages of megakaryocytopoiesis by thrombopoietin. *J Exp Med.* 1996;183(2):651-6.
10. Gurney AL, and de Sauvage FJ. Dissection of c-Mpl and thrombopoietin function: studies of knockout mice and receptor signal transduction. *Stem Cells.* 1996;14 Suppl 1:116-23.
11. Decker M, Leslie J, Liu Q, and Ding L. Hepatic thrombopoietin is required for bone marrow hematopoietic stem cell maintenance. *Science (New York, NY).* 2018;360(6384):106-10.
12. de Graaf CA, and Metcalf D. Thrombopoietin and hematopoietic stem cells. *Cell Cycle.* 2011;10(10):1582-9.
13. Wiestner A, Schlemper RJ, van der Maas AP, and Skoda RC. An activating splice donor mutation in the thrombopoietin gene causes hereditary thrombocythaemia. *Nat Genet.* 1998;18(1):49-52.
14. Ghilardi N, and Skoda RC. A single-base deletion in the thrombopoietin (TPO) gene causes familial essential thrombocythemia through a mechanism of more efficient translation of TPO mRNA. *Blood.* 1999;94(4):1480-2.
15. Ghilardi N, Wiestner A, Kikuchi M, Ohsaka A, and Skoda RC. Hereditary thrombocythaemia in a Japanese family is caused by a novel point mutation in the thrombopoietin gene. *British journal of haematology.* 1999;107(2):310-6.
16. Kondo T, Okabe M, Sanada M, Kurosawa M, Suzuki S, Kobayashi M, et al. Familial essential thrombocythemia associated with one-base deletion in the 5'-untranslated region of the thrombopoietin gene. *Blood.* 1998;92(4):1091-6.

17. Jorgensen MJ, Raskind WH, Wolff JF, Bachrach HR, and Kaushansky K. Familial thrombocytosis associated with overproduction of thrombopoietin due to a novel splice donor site mutation. *Blood.* 1998;92:205a.
18. Cazzola M, and Skoda RC. Translational pathophysiology: a novel molecular mechanism of human disease. *Blood.* 2000;95(11):3280-8.
19. Ballmaier M, Germeshausen M, Krukemeier S, and Welte K. Thrombopoietin is essential for the maintenance of normal hematopoiesis in humans: development of aplastic anemia in patients with congenital amegakaryocytic thrombocytopenia. *Ann N Y Acad Sci.* 2003;996:17-25.
20. Dasouki MJ, Rafi SK, Olm-Shipman AJ, Wilson NR, Abhyankar S, Ganter B, et al. Exome sequencing reveals a thrombopoietin ligand mutation in a Micronesian family with autosomal recessive aplastic anemia. *Blood.* 2013;122(20):3440-9.
21. Pecci A, Ragab I, Bozzi V, De Rocco D, Barozzi S, Giangregorio T, et al. Thrombopoietin mutation in congenital amegakaryocytic thrombocytopenia treatable with romiplostim. *EMBO Mol Med.* 2018;10(1):63-75.
22. Seo A, Ben-Harosh M, Sirin M, Stein J, Dgany O, Kaplelushnik J, et al. Bone marrow failure unresponsive to bone marrow transplant is caused by mutations in thrombopoietin. *Blood.* 2017;130(7):875-80.
23. Ballmaier M, and Germeshausen M. Advances in the understanding of congenital amegakaryocytic thrombocytopenia. *British journal of haematology.* 2009;146(1):3-16.
24. Ballmaier M, Germeshausen M, Schulze H, Cherkaoui K, Lang S, Gaudig A, et al. c-mpl mutations are the cause of congenital amegakaryocytic thrombocytopenia. *Blood.* 2001;97(1):139-46.
25. Ihara K, Ishii E, Eguchi M, Takada H, Suminoe A, Good RA, et al. Identification of mutations in the c-mpl gene in congenital amegakaryocytic thrombocytopenia. *Proc Natl Acad Sci U S A.* 1999;96(6):3132-6.
26. Savoia A, Dufour C, Locatelli F, Noris P, Ambaglio C, Rosti V, et al. Congenital amegakaryocytic thrombocytopenia: clinical and biological consequences of five novel mutations. *Haematologica.* 2007;92(9):1186-93.
27. Bussel JB, Cheng G, Saleh MN, Psaila B, Kovaleva L, Meddeb B, et al. Eltrombopag for the treatment of chronic idiopathic thrombocytopenic purpura. *The New England journal of medicine.* 2007;357(22):2237-47.
28. Kuter DJ, Bussel JB, Lyons RM, Pullarkat V, Gernsheimer TB, Senecal FM, et al. Efficacy of romiplostim in patients with chronic immune thrombocytopenic purpura: a double-blind randomised controlled trial. *Lancet (London, England).* 2008;371(9610):395-403.
29. Zaninetti C, Gresele P, Bertomoro A, Klersy C, De Candia E, Veneri D, et al. Eltrombopag for the treatment of inherited thrombocytopenias: a phase 2 clinical trial. *Haematologica.* 2019.
30. Bussel JB, Kuter DJ, Pullarkat V, Lyons RM, Guo M, and Nichol JL. Safety and efficacy of long-term treatment with romiplostim in thrombocytopenic patients with chronic ITP. *Blood.* 2009;113(10):2161-71.
31. Cheng G, Saleh MN, Marcher C, Vasey S, Mayer B, Aivado M, et al. Eltrombopag for management of chronic immune thrombocytopenia (RAISE): a 6-month, randomised, phase 3 study. *Lancet (London, England).* 2011;377(9763):393-402.
32. Saleh MN, Bussel JB, Cheng G, Meyer O, Bailey CK, Arning M, et al. Safety and efficacy of eltrombopag for treatment of chronic immune thrombocytopenia: results of the long-term, open-label EXTEND study. *Blood.* 2013;121(3):537-45.
33. Jurczak W, Chojnowski K, Mayer J, Krawczyk K, Jamieson BD, Tian W, et al. Phase 3 randomised study of avatrombopag, a novel thrombopoietin receptor agonist for the treatment of chronic immune thrombocytopenia. *British journal of haematology.* 2018;183(3):479-90.

34. Terrault N, Chen YC, Izumi N, Kayali Z, Mitrut P, Tak WY, et al. Avatrombopag Before Procedures Reduces Need for Platelet Transfusion in Patients With Chronic Liver Disease and Thrombocytopenia. *Gastroenterology.* 2018;155(3):705-18.
35. Bussel JB, Kuter DJ, Aledort LM, Kessler CM, Cuker A, Pendergrass KB, et al. A randomized trial of avatrombopag, an investigational thrombopoietin-receptor agonist, in persistent and chronic immune thrombocytopenia. *Blood.* 2014;123(25):3887-94.
36. Desmond R, Townsley DM, Dumitriu B, Olnes MJ, Scheinberg P, Bevans M, et al. Eltrombopag restores trilineage hematopoiesis in refractory severe aplastic anemia that can be sustained on discontinuation of drug. *Blood.* 2014;123(12):1818-25.
37. Olnes MJ, Scheinberg P, Calvo KR, Desmond R, Tang Y, Dumitriu B, et al. Eltrombopag and improved hematopoiesis in refractory aplastic anemia. *The New England journal of medicine.* 2012;367(1):11-9.
38. Oshima Y, Yuji K, and Tojo A. Eltrombopag in refractory aplastic anemia. *The New England journal of medicine.* 2012;367(12):1162; author reply 3.
39. Townsley DM, Scheinberg P, Winkler T, Desmond R, Dumitriu B, Rios O, et al. Eltrombopag Added to Standard Immunosuppression for Aplastic Anemia. *The New England journal of medicine.* 2017;376(16):1540-50.
40. Kuter DJ, and Rosenberg RD. The reciprocal relationship of thrombopoietin (c-Mpl ligand) to changes in the platelet mass during busulfan-induced thrombocytopenia in the rabbit. *Blood.* 1995;85(10):2720-30.
41. Fielder PJ, Gurney AL, Stefanich E, Marian M, Moore MW, Carver-Moore K, et al. Regulation of thrombopoietin levels by c-mpl-mediated binding to platelets. *Blood.* 1996;87(6):2154-61.
42. Nagata Y, Shozaki Y, Nagahisa H, Nagasawa T, Abe T, and Todokoro K. Serum thrombopoietin level is not regulated by transcription but by the total counts of both megakaryocytes and platelets during thrombocytopenia and thrombocytosis. *Thrombosis and haemostasis.* 1997;77(5):808-14.
43. Cohen-Solal K, Villeval JL, Titeux M, Lok S, Vainchenker W, and Wendling F. Constitutive expression of Mpl ligand transcripts during thrombocytopenia or thrombocytosis. *Blood.* 1996;88(7):2578-84.
44. Grozovsky R, Begonja AJ, Liu K, Visner G, Hartwig JH, Falet H, et al. The Ashwell-Morell receptor regulates hepatic thrombopoietin production via JAK2-STAT3 signaling. *Nature Medicine.* 2015;21(1):47-54.
45. Xu M, Li J, Neves MAD, Zhu G, Carrim N, Yu R, et al. GPIbalpha is required for platelet-mediated hepatic thrombopoietin generation. *Blood.* 2018;132(6):622-34.
46. Li Y, Fu J, Ling Y, Yago T, McDaniel JM, Song J, et al. Sialylation on O-glycans protects platelets from clearance by liver Kupffer cells. *Proc Natl Acad Sci U S A.* 2017;114(31):8360-5.
47. Wolber EM, and Jelkmann W. Interleukin-6 increases thrombopoietin production in human hepatoma cells HepG2 and Hep3B. *Journal of interferon & cytokine research : the official journal of the International Society for Interferon and Cytokine Research.* 2000;20(5):499-506.
48. Folman CC, Ooms M, Kuenen B B, De Jong SM, Vet RJWM, De Haas M, et al. The role of thrombopoietin in post-operative thrombocytosis. *British journal of haematology.* 2001;114(1):126-33.
49. Kaser A, Brandacher G, Steurer W, Kaser S, Offner FA, Zoller H, et al. Interleukin-6 stimulates thrombopoiesis through thrombopoietin: role in inflammatory thrombocytosis. *Blood.* 2001;98(9):2720-5.
50. Wolber EM, Fandrey J, Frackowski U, and Jelkmann W. Hepatic thrombopoietin mRNA is increased in acute inflammation. *Thrombosis and haemostasis.* 2001;86(6):1421-4.

51. Burmester H, Wolber EM, Freitag P, Fandrey J, and Jelkmann W. Thrombopoietin production in wild-type and interleukin-6 knockout mice with acute inflammation. *Journal of interferon & cytokine research : the official journal of the International Society for Interferon and Cytokine Research.* 2005;25(7):407-13.
52. Braakman I, and Bulleid NJ. Protein folding and modification in the mammalian endoplasmic reticulum. *Annu Rev Biochem.* 2011;80:71-99.
53. Uhlen M, Fagerberg L, Hallstrom BM, Lindskog C, Oksvold P, Mardinoglu A, et al. Proteomics. Tissue-based map of the human proteome. *Science (New York, NY).* 2015;347(6220):1260419.
54. Bonifacino JS, and Glick BS. The mechanisms of vesicle budding and fusion. *Cell.* 2004;116(2):153-66.
55. Khoriaty R, Vasievich MP, and Ginsburg D. The COPII pathway and hematologic disease. *Blood.* 2012;120(1):31-8.
56. Tang VT, and Ginsburg D. Cargo selection in endoplasmic reticulum-to-Golgi transport and relevant diseases. *J Clin Invest.* 2023;133(1).
57. Barlowe C, and Helenius A. Cargo Capture and Bulk Flow in the Early Secretory Pathway. *Annu Rev Cell Dev Biol.* 2016;32:197-222.
58. Moise Bendayan, Jurgen Roth, Alain Perrelet, and Orci L. Quantitative immunocytochemical localization of pancreatic secretory proteins in subcellular compartments of the rat acinar cell. *The Journal of Histochemistry and Cytochemistry.* 1980;28(2):149-60.
59. Kuehn MJ, Herrmann JM, and Schekman R. COPII-cargo interactions direct protein sorting into ER-derived transport vesicles. *Nature.* 1998;391(8):187-90.
60. Nina R.Salama TY, Randy W.Schekman. The Sec13p complex and reconstitution of vesicle budding from the ER with purified cytosolic proteins. *The EMBO Journal.* 1993;12(11):4073-82.
61. Balch WE, McCaffery JM, Plutner H, and Farquhar MG. Vesicular stomatitis virus glycoprotein is sorted and concentrated during export from the endoplasmic reticulum. *Cell.* 1994;76:841-52.
62. Charles Barlowe, Lelio Orci, Tom Yeung, Midori Hosobuchi, Susan Hamamoto, Nina Salama, et al. COPII: a membrane coat formed by Sec proteins that drive vesicle budding from the endoplasmic reticulum. *Cell.* 1994;77:895-907.
63. Kappeler F, Klopfenstein DRC, Foguet M, Paccaud J-P, and Hauri H-P. The recycling of ERGIC-53 in the Early Secretory Pathway. *The Journal of Biological Chemistry.* 1997;272(50):31801-8.
64. Itin C, Roche A-C, Monsigny M, and Hauri H-P. ERGIC-53 Is a Functional Mannose-selective and Calcium-dependent Human Homologue of Leguminous Lectins. *Molecular Biology of the Cell.* 1996;7:483-93.
65. William C. Nichols, Uri Seligsohn, Ariella Zivelin, Valeri H. Terry, Colette E. Hertel, Matthew A. Wheatley, et al. Mutations in the ER-Golgi intermediate compartment protein ERGIC-53 cause combined deficiency of coagulation factors V and VIII. *Cell.* 1998;93.
66. Emmer BT, Hesketh GG, Kotnik E, Tang VT, Lascuna PJ, Xiang J, et al. The cargo receptor SURF4 promotes the efficient cellular secretion of PCSK9. *Elife.* 2018;7.
67. Saegusa K, Sato M, Morooka N, Hara T, and Sato K. SFT-4/Surf4 control ER export of soluble cargo proteins and participate in ER exit site organization. *The Journal of Cell Biology.* 2018;217(6):2073-85.
68. Yin Y, Garcia MR, Novak AJ, Saunders AM, Ank RS, Nam AS, et al. Surf4 (Erv29p) binds amino-terminal tripeptide motifs of soluble cargo proteins with different affinities, enabling prioritization of their exit from the endoplasmic reticulum. *PLoS Biol.* 2018;16(8):e2005140.
69. Lin Z, Myers G, McGee B, King R, Tang V, Friedman A, et al. A Genome Scale CRISPR Screen Identifies the ER Cargo Receptor That Facilitates the Efficient Secretion of Erythropoietin. *Blood.* 2019;134.

70. Zhang B. Recent developments in the understanding of the combined deficiency of FV and FVIII. *Br J Haematol.* 2009;145(1):15-23.
71. Zhang B, Zheng C, Zhu M, Tao J, Vasievich MP, Baines A, et al. Mice deficient in LMAN1 exhibit FV and FVIII deficiencies and liver accumulation of alpha1-antitrypsin. *Blood.* 2011;118(12):3384-91.
72. Christian Appenzeller, Helena Andersson, Felix Kappeler, and Hauri aH-P. The lectin ERGIC-53 is a cargo transport receptor for glycoproteins. *Nature Cell Biology.* 1999;1.
73. Nyfeler B, Reiterer V, Wendeler MW, Stefan E, Zhang B, Michnick SW, et al. Identification of ERGIC-53 as an intracellular transport receptor of alpha1-antitrypsin. *J Cell Biol.* 2008;180(4):705-12.
74. Ordonez A, Harding HP, Marciniak SJ, and Ron D. Cargo receptor-assisted endoplasmic reticulum export of pathogenic alpha1-antitrypsin polymers. *Cell Rep.* 2021;35(7):109144.
75. Tang X, Chen R, Mesias VSD, Wang T, Wang Y, Poljak K, et al. A SURF4-to-proteoglycan relay mechanism that mediates the sorting and secretion of a tagged variant of sonic hedgehog. *Proc Natl Acad Sci U S A.* 2022;119(11):e2113991119.
76. Gomez-Navarro N, and Miller E. Protein sorting at the ER–Golgi interface. *The Journal of Cell Biology.* 2016;215(6):769-78.
77. Everett LA, Khoriaty RN, Zhang B, and Ginsburg D. Altered phenotype in LMAN1-deficient mice with low levels of residual LMAN1 expression. *Blood advances.* 2020;4(22):5635-43.
78. Zhu M, Zheng C, Wei W, Everett L, Ginsburg D, and Zhang B. Analysis of MCFD2- and LMAN1-deficient mice demonstrates distinct functions in vivo. *Blood advances.* 2018;2(9):1014-21.
79. Pecci A, and Balduini CL. Inherited thrombocytopenias: an updated guide for clinicians. *Blood Rev.* 2021;48:100784.
80. Foster DC, Sprecher CA, Grant FJ, Kramer JM, Kuijper JL, Holly RD, et al. Human thrombopoietin: gene structure, cDNA sequence, expression, and chromosomal localization. *Proc Natl Acad Sci U S A.* 1994;91(26):13023-7.
81. de Sauvage FJ, Hass PE, Spencer SD, Malloy BE, Gurney AL, Spencer SA, et al. Stimulation of megakaryocytopoiesis and thrombopoiesis by the c-Mpl ligand. *Nature.* 1994;369(6481):533-8.
82. McIntosh B, and Kaushansky K. Transcriptional regulation of bone marrow thrombopoietin by platelet proteins. *Exp Hematol.* 2008;36(7):799-806.
83. Nakamura-Ishizu A, Takubo K, Fujioka M, and Suda T. Megakaryocytes are essential for HSC quiescence through the production of thrombopoietin. *Biochem Biophys Res Commun.* 2014;454(2):353-7.
84. Nakamura-Ishizu A, Takubo K, Kobayashi H, Suzuki-Inoue K, and Suda T. CLEC-2 in megakaryocytes is critical for maintenance of hematopoietic stem cells in the bone marrow. *J Exp Med.* 2015;212(12):2133-46.
85. Sungaran R, Markovic B, and Chong BH. Localization and regulation of thrombopoietin mRNa expression in human kidney, liver, bone marrow, and spleen using in situ hybridization. *Blood.* 1997;89(1):101-7.
86. Yoshihara H, Arai F, Hosokawa K, Hagiwara T, Takubo K, Nakamura Y, et al. Thrombopoietin/MPL signaling regulates hematopoietic stem cell quiescence and interaction with the osteoblastic niche. *Cell Stem Cell.* 2007;1(6):685-97.
87. Ghilardi N, Wiestner A, and Skoda RC. Thrombopoietin production is inhibited by a translational mechanism. *Blood.* 1998;92(11):4023-30.
88. Peck-Radosavljevic M, Wichlas M, Zacherl J, Stiegler G, Stohlawetz P, Fuchsjager M, et al. Thrombopoietin induces rapid resolution of thrombocytopenia after orthotopic liver transplantation through increased platelet production. *Blood.* 2000;95(3):795-801.

89. Everett LA, Cleuren AC, Khoriaty RN, and Ginsburg D. Murine coagulation factor VIII is synthesized in endothelial cells. *Blood.* 2014;123(24):3697-705.
90. Postic C, Shiota M, Niswender KD, Jetton TL, Chen Y, Moates JM, et al. Dual roles for glucokinase in glucose homeostasis as determined by liver and pancreatic beta cell-specific gene knock-outs using Cre recombinase. *J Biol Chem.* 1999;274(1):305-15.
91. Koni PA, Joshi SK, Temann UA, Olson D, Burkly L, and Flavell RA. Conditional vascular cell adhesion molecule 1 deletion in mice: impaired lymphocyte migration to bone marrow. *J Exp Med.* 2001;193(6):741-54.
92. Wang X, Wang H, Xu B, Huang D, Nie C, Pu L, et al. Receptor-Mediated ER Export of Lipoproteins Controls Lipid Homeostasis in Mice and Humans. *Cell Metab.* 2021;33(2):350-66 e7.
93. Tang VT, McCormick J, Xu B, Wang Y, Fang H, Wang X, et al. Hepatic inactivation of murine Surf4 results in marked reduction in plasma cholesterol. *Elife.* 2022;11.
94. Khoriaty R, Everett L, Chase J, Zhu G, Hoenerhoff M, McKnight B, et al. Pancreatic SEC23B deficiency is sufficient to explain the perinatal lethality of germline SEC23B deficiency in mice. *Sci Rep.* 2016;6:27802.
95. Khoriaty R, Vasievich MP, Jones M, Everett L, Chase J, Tao J, et al. Absence of a red blood cell phenotype in mice with hematopoietic deficiency of SEC23B. *Mol Cell Biol.* 2014;34(19):3721-34.
96. King R, Lin Z, Balbin-Cuesta G, Myers G, Friedman A, Zhu G, et al. SEC23A rescues SEC23B-deficient congenital dyserythropoietic anemia type II. *Sci Adv.* 2021;7(48):eabj5293.
97. Khoriaty R, Hesketh GG, Bernard A, Weyand AC, Mellacheruvu D, Zhu G, et al. Functions of the COPII gene paralogs SEC23A and SEC23B are interchangeable in vivo. *Proc Natl Acad Sci U S A.* 2018;115(33):E7748-E57.
98. Khoriaty R, Vogel N, Hoenerhoff MJ, Sans MD, Zhu G, Everett L, et al. SEC23B is required for pancreatic acinar cell function in adult mice. *Mol Biol Cell.* 2017;28(15):2146-54.
99. Lin Z, King R, Tang V, Myers G, Balbin-Cuesta G, Friedman A, et al. The Endoplasmic Reticulum Cargo Receptor SURF4 Facilitates Efficient Erythropoietin Secretion. *Mol Cell Biol.* 2020;40(23).
100. Costantini LM, Baloban M, Markwardt ML, Rizzo MA, Guo F, Verkhusha VV, et al. A palette of fluorescent proteins optimized for diverse cellular environments. *Nat Commun.* 2015;6:7670.

Figure legends

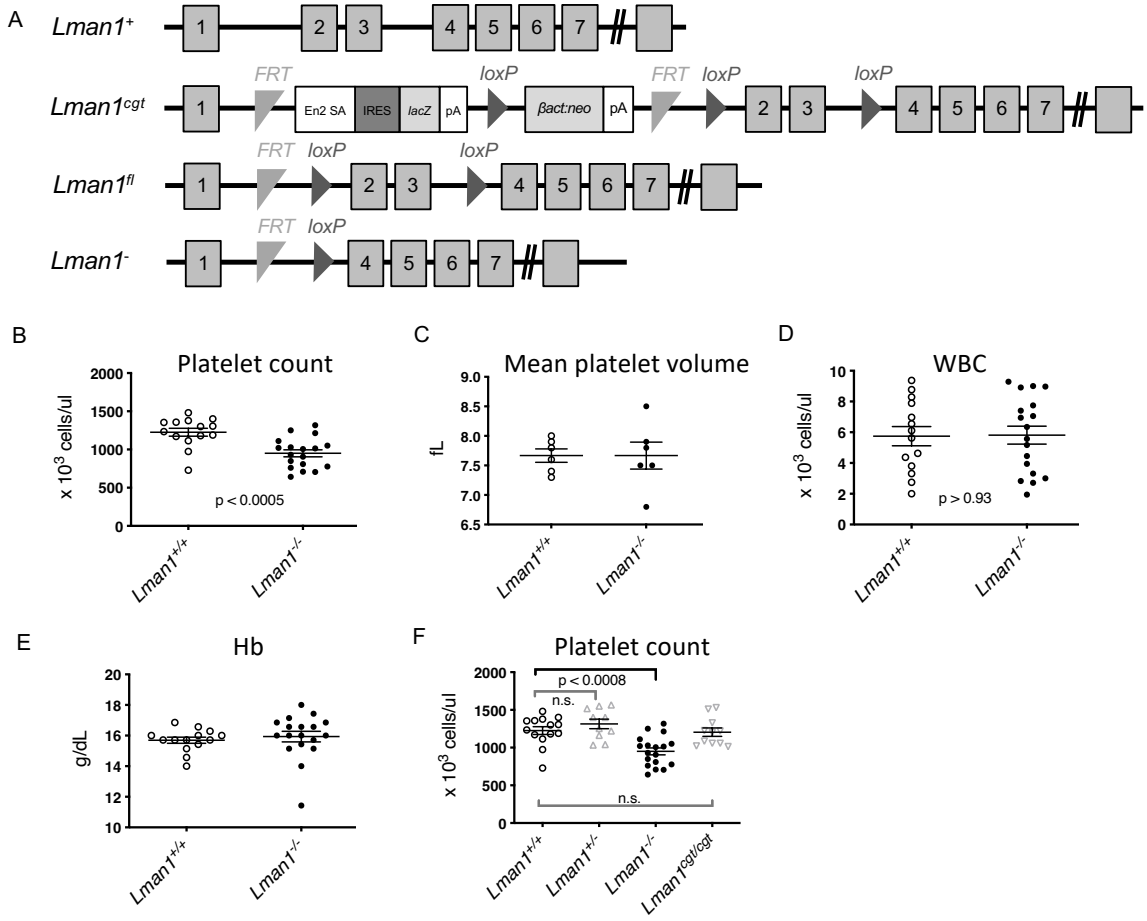

Figure 1. LMAN1 deficient mice exhibit thrombocytopenia. (A) The *Lman1* wildtype allele is denoted *Lman1*$^{+}$. The *Lman1* conditional gene-trap allele (*Lman1*^{cgt}) allele contains a conditional gene trap insertion in intron 1, which can be excised by expression of FLP recombinase. The *Lman1* floxed allele (*Lman1*^{fl}) is converted to an *Lman1* null allele (*Lman1*$^{-}$) following Cre-mediated excision of exons 2 and 3. (B-E) *Lman1*$^{-/-}$ mice exhibit (B) thrombocytopenia, (C) with normal platelet volume, and absence of (D) leukopenia or (E) anemia. Data was analyzed using unpaired Student's t-test. (F) Mice with 50% *Lman1* expression (*Lman1*$^{+/-}$ mice) or with ~7% *Lman1* expression (*Lman1*$^{cgt/cgt}$ mice) exhibit normal platelet counts. Data was compared using one-way ANOVA, with correction for multipe comparison testing.

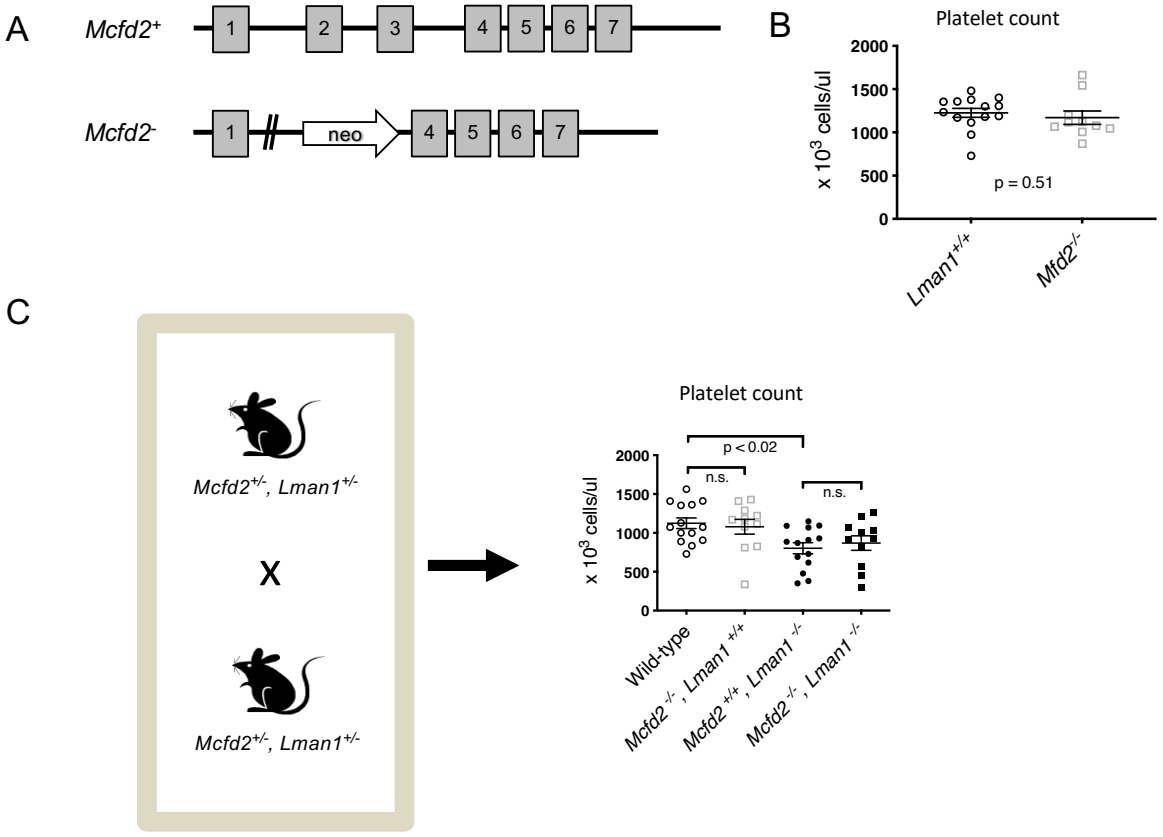

Figure 2. MCFD2 deficiency does not result in thrombocytopenia. (A) *Mcfd2*$^{-/-}$ mice were evaluated, (B) demonstrating normal platelet counts compared to littermate controls. Data was analyzed using unpaired Student's t-test. (C) LMAN1/MCFD2 double deficient mice exhibit thrombocytopenia, with platelet counts indistinguishable from *Lman1*$^{-/-}$ mice. Data was compared using one-way ANOVA, with correction for multipe comparison testing.

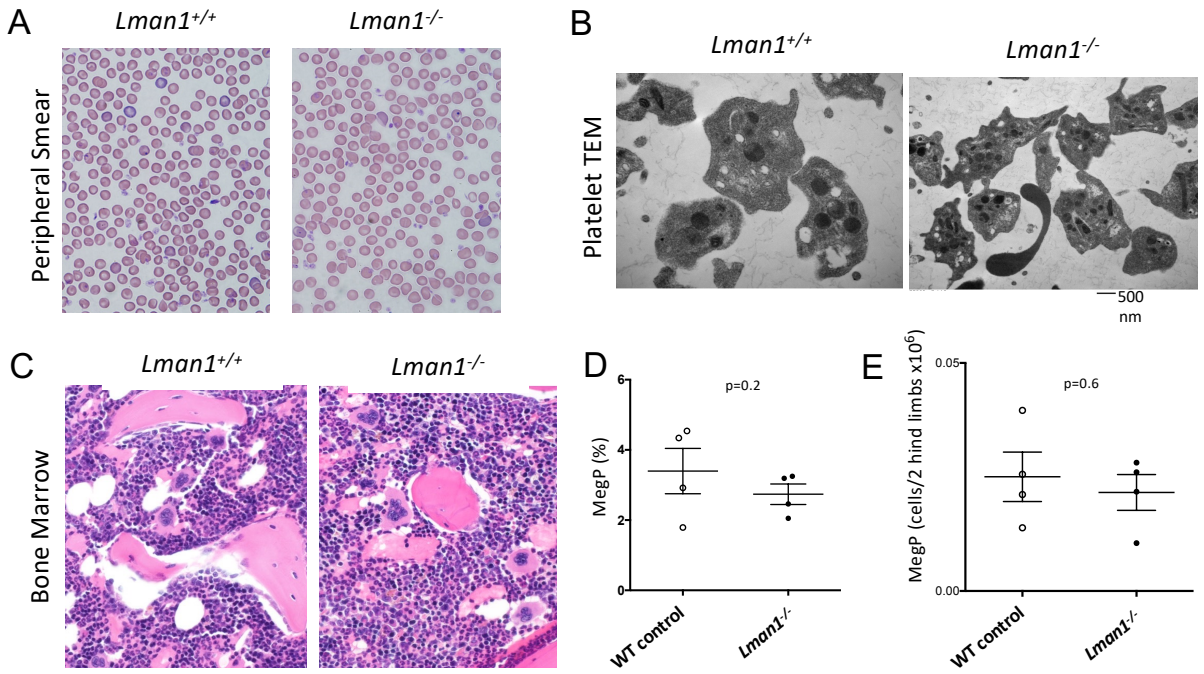

Figure 3. Megakaryocyte and platelet morphology in LMAN1 deficient mice. (A-B) LMAN1 deficient mice exhibit (A) normal platelet size and morphology by peripheral smear evaluation and (B) normal platelet dense and alpha granule morphology by transmission electron microscopy. (C) Bone marrow histology demonstrates no difference in megakaryocyte morphology between both genotypes. (D) Percentages and (E) numbers of bone marrow megakaryocyte progenitors ($Lin^-Sca^-KIT^+CD150^+CD41^+$) in LMAN1 deficient compared to littermate control mice by flow cytometry. Data was analyzed using unpaired Student's t-test.

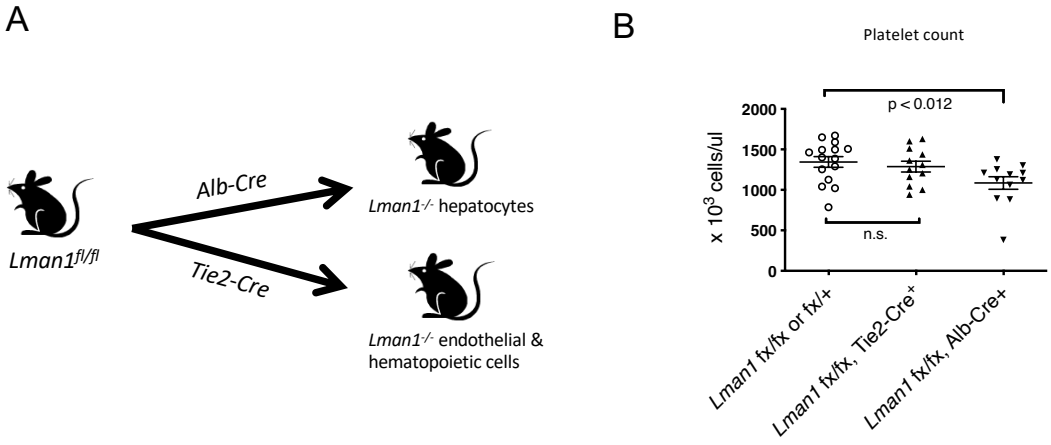

Figure 4. Deletion of *Lman1* in hepatocytes, but not hematopoietic cells, results in thrombocytopenia. (A) *Lman1* was deleted in hematopoietic cells using the *Tie2*-Cre transgene and in hepatocytes using the *Alb*-Cre transgene. (B) Mice with hematopoietic *Lman1* deletion exhibit normal platelet counts, comparable to those of wildtype litter mate controls. Hepatocyte-specific *Lman1* deletion (using the *Alb*-Cre transgene) resulted in thrombocytopenia, with platelet counts indistinguishable from those seen in mice with germline *Lman1* deletion. Data was analyzed using one-way ANOVA, with correction for multipe comparison testing.

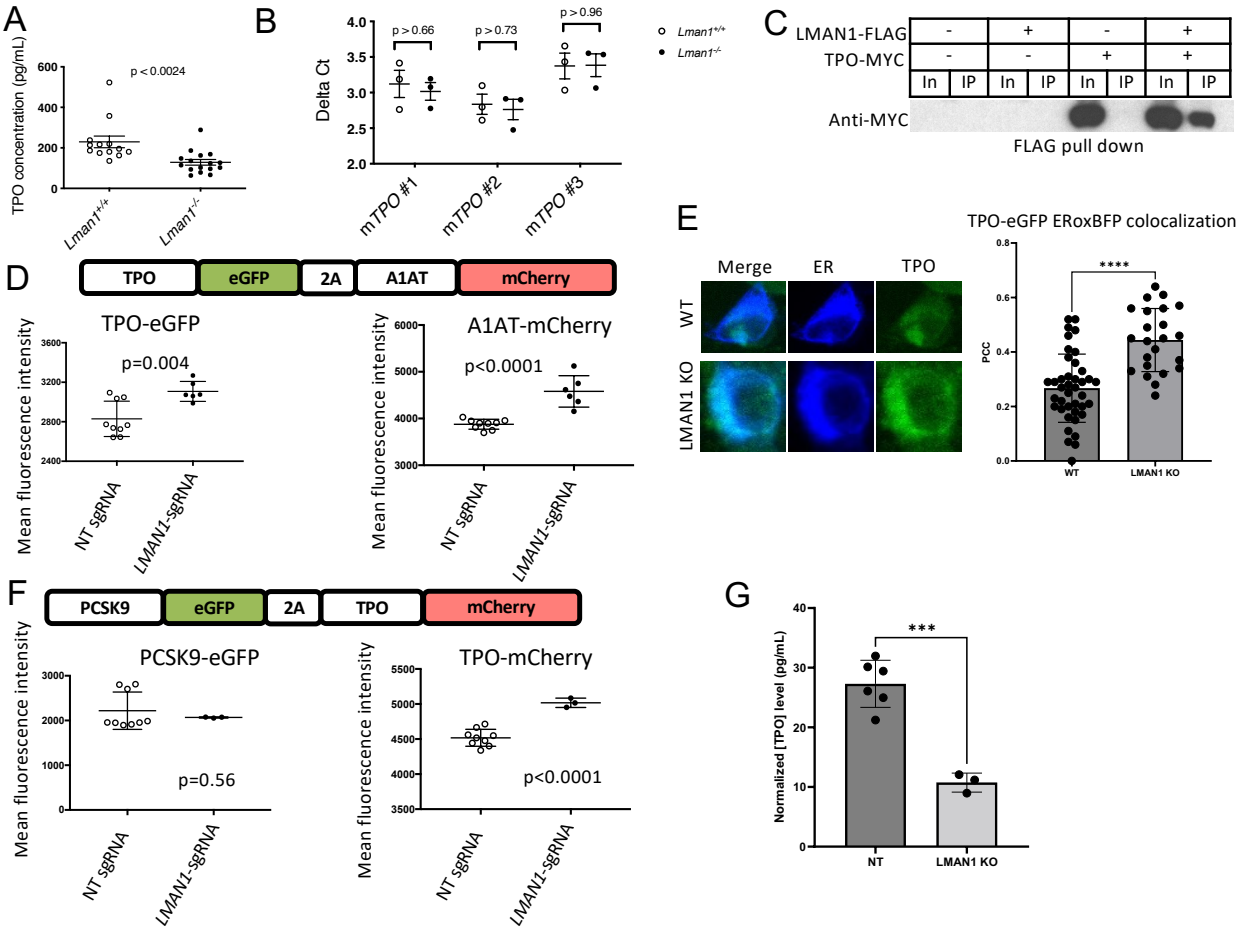

Figure 5. LMAN1 mediates the efficient secretion of TPO. (A) Plasma TPO level is reduced in LMAN1 deficient compared to wildtype littermate control mice. (B) *Tpo* mRNA levels were indistinguishable between *Lman1*$^{-/-}$ and wildtype control mice, as demonstrated using 3 different *Tpo* primer sets. (C) FLAG-tagged LMAN1 (LMAN1-FLAG) and myc-tagged TPO (TPO-myc) were expressed in HEK293T cells. A physical interaction between TPO and LMAN1 was suggested, as an anti-FLAG antibody co-immunoprecipitated TPO-myc. In, input (10%); IP, immunoprecipitated fraction. (D-E) A reporter human HEK293 cell line that expresses eGFP-fused TPO and mCherry-fused A1AT was generated. (D) Deletion of *LMAN1* using an *LMAN1* targeting sgRNA resulted in intracellular accumulation of TPO and A1AT compared to cells transduced with a non-targeting (NT) sgRNA. (E) Immunofluorescence microscopy demonstrates significantly increased colocalization of TPO in the ER (labeled with BFP) in cells transfected with *LMAN1*-targeting sgRNA (LMAN1 KO) compared to control cells (WT). PCC; Pearson correlation coefficient.**** p<0.0001. (F) A reporter cell line expressing TPO fused to mCherry and PCSK9 fused to eGFP was generated. *LMAN1* deletion results in intracellular accumulation of TPO but not PCSK9. (G) *LMAN1* deletion (LMAN1 KO) in HEP3B cells treated with 80 ng/mL IL-6 results in reduced TPO in the supernatant compared to control cells transduced with non-targeting (NT) sgRNA.*** p<0.001. Statistical analyses in this figure were performed using unpaired Student's t-test.

Tables

Crosses	Genotype Distribution at 3 weeks				p-value (χ^2)
	Lman1$^{fl/+}$, *Cre*$^{-}$	*Lman1*$^{fl/+,}$ *Cre*$^{+}$	*Lman1*$^{fl/fl}$, *Cre*$^{-}$	*Lman1*$^{fl/fl}$, *Cre*$^{+}$	
Expected %	25%	25%	25%	25%	
Lman1$^{fl/fl}$ x *Lman1*$^{fl/+}$, *Alb-Cre*$^{+}$	24% (17)	25% (18)	19% (14)	32% (23)	0.5 (n.s.)
Lman1$^{fl/fl}$ x *Lman1*$^{fl/+}$, *Tie2-Cre*$^{+}$	19% (16)	28% (23)	26.5% (22)	26.5% (22)	0.7 (n.s.)
The chi-squared test (df = 3) was based upon an expected genotype ratio of 3:1, with *Lman1*$^{fl/fl}$ Cre^{+} mice expected to represent 25% of the offspring from each mating, and all other genotypes cumulatively accounting for 75% of offspring.					

Table 1. Mouse crosses. Mice with hematopoietic/endothelial *Lman1* deletion and mice with deletion of *Lman1* in hepatocytes were viable and observed in the expected Mendelian ratios at weaning.